REPORT DOCUMENTATION PAGE

Form Approved OMB No. 0704-0188

1. AGENCY USE ONLY (Leave blank)	2. REPORT DATE	3. REPORT TYPE AND DATES COVERED
	1994	Final Report

4. TITLE AND SUBTITLE

Response of Heterogeneous Materials to the Impact Loading

5. FUNDING NUMBERS

F6170893W00982

6. AUTHOR(S)

G.I. Kanel

7. PERFORMING ORGANIZATION NAME(S) AND ADDRESS(ES)

Department of Civil Engineering
University of Surrey

8. PERFORMING ORGANIZATION REPORT NUMBER

SPC-93-4073

9. SPONSORING/MONITORING AGENCY NAME(S) AND ADDRESS(ES)

EOARD
PSC 802 BOX 14
FPO AE 09499-0200

10. SPONSORING/MONITORING AGENCY REPORT NUMBER

SPC-93-4073

11. SUPPLEMENTARY NOTES

12a. DISTRIBUTION/AVAILABILITY STATEMENT

Approved for public release; distribution is unlimited.

12b. DISTRIBUTION CODE

A

13. ABSTRACT (Maximum 200 words)

2 dimensional and 1 dimensional computer simulations of shock-wave phenomena and uniform high-rate deformation in composite, porous and brittle materials have been performed. A resonance regime of shock compression of 1-D laminated model of the composite is discussed. An empirical constitutive relationship has been constructed to describe the dispersive effects in a composite in continuous manner. Computer simulation of dynamic compaction shows changing symmetry of pores. The formulation of shear bands of various configurations with friction and without friction was analyzed in two-dimensional geometry.

14. SUBJECT TERMS

15. NUMBER OF PAGES

55

16. PRICE CODE

N/A

17. SECURITY CLASSIFICATION OF REPORT	18. SECURITY CLASSIFICATION OF THIS PAGE	19. SECURITY CLASSIFICATION OF ABSTRACT	20. LIMITATION OF ABSTRACT
UNCLASSIFIED	UNCLASSIFIED	UNCLASSIFIED	UL

RUSSIA ACADEMY OF SCIENCES

HIGH ENERGY DENSITY RESEARCH CENTER,

RESPONSE OF HETEROGENEOUS MATERIALS TO THE IMPACT LOADING.

by

V.E.Fortov, V.I.Galburt, M.F.Ivanov, G.I.Kanel, A.N.Parshikov

Contract SPC-93-4073

(Final report)

Principal investigator: G.I.Kanel

October 3, 1994

RUSSIA ACADEMY OF SCIENCES

HIGH ENERGY DENSITY RESEARCH CENTER,

RESPONSE OF HETEROGENEOUS MATERIALS TO THE IMPACT LOADING.

by

V.E.Fortov, V.I.Galburt, M.F.Ivanov, G.I.Kanel, A.N.Parshikov

Contract SPC-93-4073

(Final report)

Principal investigator: G.I.Kanel

October 3, 1994

Abstract:

2-dimensional and 1-dimensional computer simulations of shock-wave phenomena and uniform high-rate deformation in composite, porous and brittle materials have been performed. A resonance regime of shock compression of 1-D laminated model of the composite is discussed. An empirical constitutive relationship has been constructed to describe the dispersive effects in a composite in continuous manner. Computer simulation of dynamic compaction shows changing symmetry of pores. The formation of shear bands of various configurations with friction and without friction was analyzed in two-dimensional geometry. It has been shown the shear bands can be responsible for the multi-wave structure forming at shock compression of brittle material. The constitutive model of brittle material has been proposed and tested in series of 1-D hydrodynamic calculations. The model includes two parallel elements. One of them works as an usual elastic-plastic body, another element describes the friction and dilatancy in the comminuted component. The comminuted component fraction is a scalar damage variable which grows from a value of 0 to 1 as a result of inelastic deformation of the intact component.

1. INTRODUCTION

Ceramics, composite and porous materials are widely used as structural materials in the space and rocket technology. To predict consequences of intense attacks like micrometeorit impacts, it is necessary to describe the behavior of similar materials under shock-wave loading. Usual way to analyze such phenomena is its computer simulation where materials properties are described by equations of state and constitutive relationships. Current hydrocode modeling capabilities are confined almost exclusively to homogeneous isotropic media and deal with a macroscopic continuum. It seems that constitutive relationships for routine using in hydrocodes have to be continual also.

For heterogeneous materials, which consist of two or more phases, several factors complicate constitutive relation constructing. Response of such kind of materials is determined by behavior of individual components as well as their interactions and has to depend on the space distribution of components in the material. A characterization of the dynamic behavior of heterogeneous material requires more profound understanding of the phenomena. Current hydrocode modeling capabilities are confined almost exclusively to homogeneous isotropic media and deal with a macroscopic continuum. It seems that final constitutive relationships for routine using in hydrocodes have to be continual also. On the other hand, a computer simulation of processes in model heterogeneous materials can give a necessary information to construct these relationships.

The main objective of this work is the analysis and description of the behavior of composite, porous and brittle materials under impact loading. The goal is to construct models of heterogeneous materials and constitutive relationships for computer simulation of impact phenomena. The work includes two-dimensional computer simulation of deformation processes in models of these heterogeneous materials. Two-dimensional computer simulation gives a detailed picture of the process on the microscopic level. Results of the simulations are then used to construct constitutive relationships that are incorporated then into the hydrodynamic codes.

The Part 2 of this report presents the state of the problem. It includes a literature overview of experimental and theoretical results in field of response of composite, porous and brittle materials to the impact loading and some analysis of compressibility of mixtures. Part 3 presents results of 2-D computer experiments. Part 4 contains constitutive models and data of 1-D calculations. Mathematical models and codes are described in Appendix.

2. BACKGROUND AND LITERATURE OVERVIEW

2.1. COMPOSITE MATERIALS CONTINUUM MODELS.

Series of simplified approaches have been developed to describe a viscous-elastic behavior of composite materials at low and moderate strain rates [1-4]. These approaches are based on various methods of the mechanical parameters averaging. For example, effective modules theory [1,2] uses assumption that average stresses $\bar{\sigma}_{ij}$ and average strains $\bar{\varepsilon}_{ij}$ are related by the Hooke's low through the effective modules C_{ijkl}

$$\bar{\sigma}_{ij} = C_{ijkl}\bar{\varepsilon}_{ij}$$

Effective modules depend on elastic properties of components as well as on the geometrical form and space distribution of components. This theory is based on an approach that all components of stress tensor and strain tensor averaged in some volume are equal to corresponding tensor components for composite material taken as a whole. Effective toughness theory and its modifications are used for description of composites with fibers. It is assumed the fibers-matrix interaction occurs due to matched displacement of fiber axis and matrix. Kinetic and potential energies of the composite deformation are the sum of corresponding energies of the composite components, which are taken with weights assigned in according to volume fraction of components. Anisotropic model of composite materials involving strength effects is discussed in ref. [5].

In conditions of shock-wave loading materials work mainly in the plastic deformation region. As a result, many factors considered in theories mentioned above have an insignificant influence on the

dynamics of media. On the other hand, these theories are based, as a rule, on the acoustic approach and can not be applied for description of intense dynamic loading. An additional factor of the impact loading of composites is the acoustic interaction between matrix and fibers. Wave reflections between components of the material occur as a result of their different dynamic impedances. Wave reverberations produce a dispersion of a load pulse in the matter. This leads to changing attenuation of the load and has to be taken into account at analysis of hypervelocity impact phenomena. In order to calculate the composite material response to shock-wave loading, it is necessary to have in computer code an equation of state of the material and constitutive relations describing dispersion properties of the material.

2.2. SHOCK COMPRESSIBILITY OF COMPOSITE MATERIALS.

The shock compressibility of mechanical mixtures of two materials with known Hugoniots is calculated as a sum of the components compressibilities [6]. According to this additive approach, the specific volume V of mixture under pressure P is

$$V(P) = \alpha\, V_1(P) + (1 - \alpha)\, V_2(P),$$

where α is the mass fraction of first component in the mixture, $V_1(P)$ and $V_2(P)$ are specific volumes of components under pressure P. The most consistent consideration of shock compressibility of two-component mixture has been done by G.E.Duvall and S.M.Taylor [7]. As a rule, the thermal equilibrium is not reached in real situations. Fortunately, wave propagation is not very sensitive to thermal effects in the moderate pressure region. Comparison of additive calculations with experimental data [6] shows reasonably well agreement between measured and calculated Hugoniots of mixture when Hugoniots of components were used to calculate $V_1(P)$ and $V_2(P)$. Then the shock front velocity and other kinematic parameters of shock waves in the mixture are determined through the Hugoniot. Some formal approximate equation of state can be constructed also using the $P(V)$ Hugoniot of the mixture [8]. Calculations of compressibility of the mixture using the mixture theory [9] or some mechanical models [10] are much more

complicated but provide approximately the same results.
In frames of additive approach the bulk sound velocity in mixture C is formally calculated through known bulk sound velocities in components using relationship

$$\frac{dV}{dP} = \alpha \frac{dV_1}{dP} + (1-\alpha) \frac{dV_2}{dP} = - \frac{V^2}{C^2} \qquad (1)$$

Thus, a square of the initial bulk sound velocity in mixture is calculated as

$$C^2 = \frac{V^2}{\alpha / \rho_1^2 C_1^2 + (1-\alpha)/\rho_2^2 C_2^2} \qquad (2)$$

It is interesting to mention that sound velocity value for mixture can be less then sound velocity values for both components. Figure 1 shows the sound velocity of a aluminum/tungsten mixture calculated as a function of the tungsten mass fraction. The dependence has a minimum near 0.9 mass fraction of tungsten. Another interesting point is a relationship between a shock front velocity and a particle velocity in mixtures. It is known this relationship is, as a rule, linear one for metals, alloys and other individual matters. Figure 2 shows Hugoniots of mechanical mixtures of tungsten/aluminum, tungsten/epoxy and aluminum/epoxy calculated for volume fraction of heavy component equal to 0.375 using linear Hugoniots of all components. One can see Hugoniots of mixtures are not exactly linear but curvature is not significant.

2.3. POROUS MATERIALS

The initial stage of the compression of a porous body is characterized by elastic strains. The yield strength decreases with increasing initial porosity of the medium. Irreversible compaction occurs above the elastic limit. The load required to produce a given density is found to increase with decreasing initial density of the body. This is explained by strain hardening of grains in the material during the process of compaction. Removal of the load is not accompanied by a large change in porosity. Complete compaction of porous material is attained at compression stress, which is somewhat higher than the Hugoniot elastic limit for solid material.

Several constitutive models were developed to describe a behavior of the porous media through the solid materials properties and some mechanics of a shock wave interaction with pores. Each model contains several free parameters or material constants that can be determined only by fitting these models to experimental Hugoniot data. The compaction models have frequently been formulated by solving the stress-strain relationships in a specific porous geometry. A theoretical prediction of the unique equilibrium compaction relation requires detailed knowledge on material property, pore collapsing mechanism, and microscopic stacking geometry of matrix material.

One from first models of porous body is so-called p-α model of W.Herrmann [10]. Parameter of porosity α in this model is the ratio of the pores specific volume V to the specific volume of solid matrix V_m. A total volume of the porous mater under stress is changing due to closing pores and due to changing volume of the matrix. The Herrmann's relationship for porosity is

$$\alpha = 1 + (\alpha_Y - 1)[(p_s - p)/(p_s - Y_p)]^2,$$

where α_Y is a porosity value at the yield stress, p_s is the pressure of complete compaction, Y_p is yield stress for the incipient porous material. A thermodynamic equation of state for porous material $p = p(V/\alpha, E)$ is the same like one for the solid material.

R.R.Boade [11] has found that the exponential p-α model fits experimental data more accurately. The exponential p-α model was given by

$$\alpha = 1 + (\alpha_Y - 1)e^{-\hat{\alpha}(p-p_1)},$$

where $\hat{\alpha}$ and p_1 are the fit constants.

M. Carroll and A. Holt [12] used an equation of state in the form $p = \alpha^{-1} f(V/\alpha, E)$ which takes into account decreasing area in the body cross-section of the pressure acting due to the porosity.

A simple constitutive model for the shock Hugoniot of porous materials in the incomplete compaction regime was developed in ref. 13. The model is based on the assumptions that: (1) the compacted powder geometry in the incomplete compaction regime is

approximately similar for the shock compaction and the quasi-isostatic compaction, and (2) the net effect of the strain rate and the high temperature developed in the shock compaction results in a material strength whose magnitude is similar to that appearing in the case of the quasi-isostatic compaction. With these assumptions the constitutive relationship has been obtained in the following form:

$$V = V_s(p)\left[1 + \left(\frac{V_{oo}}{V_o} - 1\right)e^{-(5n-9.4)(p-\sigma_y)}\right],$$

where $V_s(p)$ is a specific volume of solid matrix as a function of pressure, V_{oo} and V_o are initial specific volume values for porous and solid materials, $n \approx 2.1$ to 2.5 is the Meyer work-hardening index of solid material defined from hardness measurements at different loads, σ_y is yield strength of the porous material.

Models described above do not consider a stress relaxation during compacting. In the ref. 14 by Carroll and Holt some simple kinetics of the spherical pores collapsing was incorporated into the model using the Maxwell's viscosity:

$$\dot{\alpha} = M(\alpha)\left[\dot{p} + \frac{p - p_o(\alpha)}{\tau}\right],$$

where $M(\alpha)$ is a function describing an elastic behavior of α, $p_o(\alpha)$ is an equilibrium pressure for given α value. Ansamble of spheres with radius b_o each of them contained an internal void with radius a_o was considered. The porosity α is related with a_o, b_o through the relationship

$$(b_o/a_o)^3 = \alpha_o/(\alpha_o - 1).$$

According to this model, the relaxation time τ is proportional to the pore size a_o:

$$\tau = [\rho a_o^2 \ (3Y(\alpha_o - 1)^{2/3}]^{1/2},$$

where ρ is the solid matrix density, Y is yield stress of the matrix. Results of computer simulation of the porous aluminum with this model and work-hardening incorporated to it (ref. 15) show generally good agreement between theory and experiment, including

both quasistatic and shock data. It has been shown the viscosity is more important to describe the shock front rise time than size of pores. An adequate description of the width of a steady compression wave in porous aluminum was achieved by using viscosities in the range 1-10 Pa s.

Model of Carroll and Holt was developed in ref. 16 with more careful description of viscosity and dynamics of pores collapse. Two material parameters $K = (1/D)(Y/\rho_o)^{1/2}$ and $R = \eta/[\alpha_o (Y\rho_o)^{1/2}]$ allows to analyze the behavior of mater over a wide range of stresses and material properties.

Following development of model has been done in ref. 17 through the incorporation of deviatoric stresses into the model. It has been done by such a way that porosity and evolution of the pores form is determined not only by pressure but by full tensor of stresses. According to model, pores can be closed even by shear stresses only. The constitutive relationship is based on the conception of the yield surface in the space of stresses which is varied as a function of the porosity α.

The shock compression of porous media produces greater heating of the medium than the shock compression of solid materials. The distribution of dissipated shock energy in the medium depends mainly on how the pores are collapsed during compression. The porous-body model, simulated by a set of steel balls, has been used in ref. 18 to show that the deformation produced during the impact compression of a porous body is localized mostly near the surface of granules. The theoretical analysis of viscoplastic heating of matter in the neighborhood of collapsing spherical pores was carried out in refs. 19 to 22. A micro-level numerical simulation shows the overheating matter near the pores at shock compression also. It was demonstrated in calculations of Mader [23] of shock-wave propagation in liquid media containing closed cavities. The shock-wave interaction with density discontinuities leads to formation of regions of high temperatures. The size of similar "hot spots" is close to initial diameter of pores. The same effect was observed in ref. 24 where consolidation of composite material and evolution of the particles form at shock compression were analyzed.

2.4. BRITTLE MATERIALS

The high-strain-rate behavior of ceramics and other brittle materials has more individual peculiarities than do metals. Different modes of a brittle materials deforming under compressive and shear stresses are illustrated schematically in Figure 3. Oxides and intermetallic compounds have a very high energy of nucleation of dislocations which are responsible for the plastic deformation mechanisms of metals and other ductile crystalline materials. Instead of dislocations, inelastic deformation of brittle materials is governed by the cracking. At low pressure the shear cracks and cracks oriented parallel to the compression direction nucleate under stresses of 1/3 to 2/3 of the elastic limit [25]. The cracking is accompanied with some small volume increment, - so called dilatancy, of order of 1% or less.

A number of physical mechanisms [25] are responsible for the dilatational response of brittle materials at triaxial compression tests. They include, for example, the opening of secondary cracks, void growth in the vicinity of the crack tips resulting from a locally tensile stress field, and void opening at the intersections of cracks. In the case of granular materials, compressional dilatancy may result simply from a loss of closed compactness. Initially separate micro-cracks are not united and do not cause the body fracture on the whole. The growth and collision of cracks at following increasing shear stresses produce a fracture of the material. If pressure is high enough, a plastic deforming requires less energy than cracking and brittle materials become ductile.

A deformation of solids in shock waves is one-dimensional one and shear stresses arise simultaneously with increasing pressure. Depending on a relation between elastic modules and the cracking threshold as a function of pressure, the state of material can pass through the dilatation area or come directly to the area of plastic deformation. It seems, both these cases were observed in series of experiments with plane-shock-wave loading of different ceramics performed during last decade.

Most advanced and informative measurements of shock compression

and release in high-strength ceramics were performed by M.E.Kipp and D.E.Grady [26-28]. The shock load/unload profiles of silicon carbide, titanium diboride, boron carbide and zirconium dioxide ceramics subject to plate impact provide distinctive features of the material response that can be used in the formulation and development of constitutive models. Important results were obtained also by the group of Z.Rosenberg, S.Bless, and N.S.Brar [29-31] and D.P.Dandekar et al. [31-33] for the alumina and titanium diboride, W.-D. Winkler and A.J.Stilp [34] for alumina, titanium diboride, silicon carbide, and boron carbide. These groups measured also the spall strength at shock intensities below and above the Hugoniot elastic limit and deviator stresses in shock-compressed ceramics. The post-test examination of recovered ceramic samples was carried out [32,33,35,36].

Results of experiments with ceramics exhibit all possible load ways shown in Fig.3. For example, stress-strain diagram of the silicon carbide is typical for elastic-plastic materials; shock compression of the boron carbide ceramics is accompanied with cracking and, as a consequence, with decreasing shear strength; it seems the behavior of the titanium diboride is some intermediate between former two cases with crack nucleation start below the elastic limit and obvious elastic-plastic following behavior.

The theories called usually the damage continuum mechanics are widely used for phenomenological description of high-strength brittle material response [37-44]. The state of material element (for simplicity, in isothermal approximation) is characterized by $\mathbf{e}$ - total strain tensor, $\mathbf{e}^{\mathbf{p}}$ - plastic (or viscous) strain tensor, w - tensor's or scalar parameter of damage. Being the material reaction, the stress tensor is supposed to be a function of actual strains and damage, i.e.

$$\sigma = \sigma(\mathbf{e}, \mathbf{e}^{\mathbf{p}}, w)$$

System of constitutes equations is also including the law of plastic (viscous) flow

$$d\mathbf{e}^{\mathbf{p}}/dt = \Psi(\sigma, \mathbf{e}^{\mathbf{p}}, w)$$

and an equation of a damage evolution

$$dw/dt = \Omega(\sigma, e^p, w)$$

In case of rate-independent materials the functions Ψ and Ω depends also on the rate of σ changing. Relationships (2), (3) connect rates of the plastic strain and damage evolution with the actual state of material element. The second group of essential assumptions includes the suppositions concerning to existence of yield surface and damage one, gradientality (or nongradientality) of plastic flow and damage evolution process etc. The phenomenological description of damaged materials is connected with definition of damage measure.

Series of attempts to construct reasonable constitutive model for description of response of hard ceramics are known. F.L.Addessio and J.N.Johnson [45] are developing a microphysically based model of the brittle materials inelastic deformation by cracking, which includes the progressive loss of strength and degradation of shear module as well as the post-failure response of a granular material with friction. Crack instability conditions and inelastic strains are obtained by considering the response of individual micro-cracks to an applied stress field. Similar model of D.J.Grove and A.M.Rajendran [46] assumes preexisting randomly distributed microcracks in ceramics, plastic flow above the yield strength, degradation of elastic modules and strength due to microcracking under both compression and tension. D.Steinberg [47] has performed a computer simulation of the shock-wave processes in ceramics with phenomenological approach which was successfully used earlier for metals. He described the yield strength as a function of the pressure, temperature, strain and strain rate. The description includes also the simplest form of the Cochran-Guinan Baushinger model [48] with degrading shear module at reverse deformation. The phenomenological model with the damage softening term was used also in calculations of J.F.Davis et al. [49]. The damage evolution was assumed to be a function of the plastic work rate in compression only.

One have to say that good agreement between results of computer simulation and experimental profiles takes place just for rather elastic-plastic materials like the silicon carbide. This does not take a place for the materials, like boron carbide, which are

crushed under compression with the shear component. It seems the advanced model should include both the strain hardening and softening, Baushinger effect, dilatancy and a factor of the strain rate.

3. RESULTS OF 2-D COMPUTER EXPERIMENTS.

Computer simulation of the heterogeneous materials response to impact loading has been carried out with 2-D Lagrangian code on triangular grid. The mathematical model is described in Appendix A.

3.1. 2-D SIMULATION OF SHOCK WAVES IN A COMPOSITE MATERIAL.

On the first stage we studied in the hydrodynamic approach the dissipative properties of aluminum reinforced by tungsten fibers. With this goal 2-D computer simulation of steady shock waves in the composite has been performed. Steady shock waves are most convenient for interpretation and analysis because the strain rate, the rate of a longitudinal stress increase, and deviator stresses are related by simple dependencies in this case.

Dimensions of triangular Lagrangian grid were 200x40 with the 5 μm initial size of cells. The volume fraction of hexagonally placed tungsten fibers was equal to 0.375. The average diameter of tungsten fibers was 60 μm. A cross-section of fibers at the triangular grid was approximated by hexagons. Rectangular shock pulses of various intensities were introduced into the material through the left boundary by linear increasing its velocity or pressure. Due to limited computer resources, it is practically impossible to calculate with high resolution the steady wave buildup from the initial shock jump. In order to have a possibility of calculations with small cells of the grid and to keep an accuracy of calculations, we have performed series of calculations with varied rise time of the incipient load pulse. Results of calculations were internal deformation of the material and longitudinal stress profiles in different moments of time.

An example of the digitized microstructure after shock compression is shown in Fig. 4. Figure 5 shows an example of integral pressure (longitudinal stress) profiles which were constructed by averaging pressure values in cells of greed, including viscous components,

along series of cross-sections perpendicular to the load direction. The weight averaging was done taking into account the fraction of crossed cell. Due to limited amount of fibers in the composite and to finite grid dimensions the calculated pressure profiles are not monotonous. It is necessary to mention that in case of pure aluminum the compression wave evolution was monotonous and the calculated minimal shock-front thickness was approximately equal to 4 or 5 cell sizes, that is 20-25 μm. The compression wave thickness is much more in the case of composite materials. This means the numerical and approximation viscosities do not have any essential contribution into the digitized rise times for the composite material case.

Calculations with the initial rise time 100 ns provide the steady compression wave buildup at 1 mm of the propagation distance. A steadiness of the compression wave was verified through its average propagation velocity. The propagation velocity of steady wave equals to the shock front velocity calculated for the aluminum-tungsten mixture. The thickness of steady compression waves in composite amounts to several (3 to 5) periods of fibers layers and decreases gradually with increasing the shock intensity.

Figure 6 shows stress profiles which were calculated taking into account elastic-plastic properties of both matrix and fibers materials. The yield strength Y0 was 0.5 GPa for aluminum and 3 GPa for tungsten. Calculations show much more steep middle part of the compression wave in the case of elastic-plastic behavior in the low pressure range. Obviously there are two reasons of the fact: (i) an increased average sound velocity accelerates the wave reverberations; (ii) a resistance to shear strains in solids promotes to faster buildup of a final configuration of the shock-compressed composite. Only very weak precursor is observed in the case of 2-dimensional elastic-plastic composite, but the final stress exceeds the shock pressure in corresponding liquid-like material. It seems the difference in average final axial stresses is controlled by the yield strength of the matrix.

3.2. POROUS MATERIALS.

Some preliminary results for porous materials were obtained in two

modes of dynamic compaction. 2-D computer simulation was performed in the same geometry, as shown in Figure 4, with a gas placed instead of fibers in composite material. Solid component of porous matter was described as an ideal elastic-plastic body without strain-hardening.

Figure 7 shows a deformation of the grid in the initial stage (71 ns after the process start) of shock wave propagation in porous aluminum. The boundary velocity was 1 km/s. Contrary to usual models of shock compaction, one can see a non spherical closing of pores at one-dimensional shock compression.

A computer simulation permits one to study a uniform compression of the material. For this mode the uniform velocity distribution along the sample axis was used as an initial condition and the constant values of velocity (u0 for the left boundary and 0 for the right boundary) were used as the boundary conditions. Figure 8 shows the sample deformation after 80 ns at u_o = 3 km/s. In this case pores are closed more symmetrically in comparison with shock-wave compaction, but nevertheless the spherical symmetry is not kept. Figure 9 shows the average axial stress in porous tungsten as a function of strain at uniform compression. After small initial elastic part of the diagram a remarkable growth of stresses is beginning just near the end of the compaction process. Obviously this is because the strain-hardening and viscosity were not involved in calculations.

The elastic limit of one-dimensional compression is 1.9 GPa. Meanwhile the yield strength of tungsten used in calculations was 3 GPa what corresponds to 5 GPa of the Hugoniot elastic limit of solid tungsten. According to Steinberg's model [56] the elastic limit of porous tungsten was expected to be 1.70 GPa. Results of calculations some exceed preestimated value, but the discrepancy is not very large. It is possible to say that simple Steinberg's model can be quite used as a constitutive model of porous elastic-plastic body. To take into consideration the strain hardening effect, it is necessary to use modified models, like model of Ki-Hwan Oh and Per-Anders Persson [13].

3.3. 2-D SIMULATION OF SHOCK COMPRESSION OF A BRITTLE MATERIAL

The dynamic compression of brittle material was simulated in our calculations artificially as a shear bands formation in the ideal elastic-plastic body. Shear bands are formed in preliminary determined places of the sample when the stressed state in sample reached some threshold conditions (usually half of the yield strength of the main material). After that the resistance to a shear deformation inside the bands was set to be zero or was proportional to pressure like a friction. The friction coefficient was considered as a free parameter and was varied. At high pressure the friction forces can exceed the yield strength. In our calculations we limited the friction resistance to shear by the yield strength of the ceramic. An equation of state and elastic-plastic parameters of the SiC ceramic were used in all 2-D calculations.

Two series of calculations with various geometry of shear bands have been performed. An example of deformation of a brittle sample with intersecting shear bands, is shown in Figure 10. Figure 11 shows the stress-strain diagrams for samples with different frictions inside shear bands. In general, these diagrams are quite similar to observed experimentally [26,27] for ceramics. In the case of zero friction, hydrostatic states are created inside the shear bands. As a result, after the shear bands formation the structure of the solid ceramic is changed to structure of solid grains surrounded by liquid layers. As a result, the stressed state of the material on the whole becomes the hydrostatic one also. We did not see any interactions between grains and dilatancy effects in our model. In the case of non-zero friction the stressed state after the shear bands formation is controlled by the friction coefficient.

Besides the geometry shown in Fig. 10, simulations with non-crossing bands were performed at the same relative area of inclined shear bands. It was expected that in the last case the shear bands formation should not be accompanied with hydrostatic states of the matter. Figure 12 shows the calculated stress-distance profiles for the ceramic in frame of the pure elastic-plastic model (without shear bands), and in frame of the model of elastic-plastic matter with shear bands. Of course, the shear

bands formation lowers the Hugoniot elastic limit. In the case of non-zero friction, the simulation gives three-wave structure when the friction forces inside the shear bands exceed the yield strength. These three-wave structures are some similar to experimental velocity profiles measured for the titanium diboride ceramic. Qualitatively stress profiles are not changed with varying the bands geometry.

4. CONSTITUTIVE MODELS AND 1-D COMPUTER SIMULATION.

4.1. SHOCK-WAVE PROCESSES IN LAYERED COMPOSITES.

Behavior of sophisticated systems is usually investigated on simple models. Such a simple model of composite materials can be presented as a plate composed of alternating flat layers of two different materials perpendicular to the direction of shock propagation. Shock-wave phenomena in laminated composites were discussed earlier in refs. [50-52]. In this case the first shock wave decays very rapidly due to numerous waves reflections at interfaces. It has been shown the wave front induced a large amount of ringings as it passed through the layers of the composite. Obviously, the final shock-compressed state has to correspond to the Hugoniot of the mixture.

Figure 13 shows results of computer simulation of shock compression of laminated plate consisting of the copper and polyethylene layers. The pressure and particle velocity distributions at several moments of time show the resonance behavior of such periodical one-dimensional composite. The pressure (and compression) oscillations are concentrated mainly inside the soft polyethylene layers. Due to that one can expect the main dissipation has to be localized in the soft material also. The velocity oscillations are concentrated mainly at more heavy copper layers. Figure 14 shows pressure histories in the middle sections of copper- polyethylene and aluminum-polyethylene targets. One can see the pressure oscillations have an approximately constant period and are near harmonic in form. The period of oscillations approximately corresponds to the sound propagation time through two alternating layers of the composite. Wave reflections between layers smear the wave front, but its average propagation velocity is practically equal to the shock-

front velocity in the mixture calculated for a given boundary velocity. An average pressure also corresponds to the Hugoniot of the mixture. The rise time of first compression wave approximately equals the period of oscillations. The pressure oscillations can pass to a homogeneous barrier placed behind of the layered target if the dynamic impedance of the barrier is high enough.

A reality of oscillations has been examined experimentally. With this goal the pressure profile at the interface between the target, consisting from 10 copper foils 0.2 mm thick and 10 polyethylene films 0.2 mm thick, and copper plate was measured with manganin pressure gauge. The initial load pulse was triangular in form with a total duration about 20. Result of measurements presented in Figure 15 confirms an appearance of oscillation. Relatively small amplitude of measured oscillations and relatively fast decay of them are explained by the viscosity of soft polyethylene layers where a main deformation occurs.

Figure 16 shows an influence of stress relaxation in the polyethylene layers on the computed wave profiles. One can see oscillations decay much faster if the relaxation time is some less than half-period of oscillations. In the case of large relaxation time behavior of soft layers becomes closer to elastic one, what can be seen as increasing the average propagation velocity and decreasing the period of oscillations. The stress relaxation in heavy rigid layers does not produce any essential effect.

Elastic-plastic response of both components increases the wave dispersion in a composite and damps resonance oscillations. This can be seen in Fig. 17 that shows calculated pressure profiles at the interface between a tungsten barrier and the *Al/W* layered composite with the tungsten volume fraction of 0.375. The weak precursor increases the total rise time of the first compression wave and oscillations decay much faster in the elastic-plastic composite.

4.2. 1-D COMPUTER SIMULATION OF THE WAVE DISPERSION IN COMPOSITE MATERIAL.

A dispersion of shock front takes place in composite materials due to waves' reflections between components with different dynamic

impedances. Comparison of the wave propagation characteristics of composite and viscous (i.e., stress relaxing) materials reveals that there are some basic similarities in their wave profiles. Composite and viscous materials appear to sustain the steady wave. The smooth wave transitions in viscous materials, which are attributable to rate effects, appear to be similar to smooth wave transitions in the composite which are attributable to dispersive effects. In view of this similarity the gross behavior of a composite can be described by an appropriate viscous material constitutive model, even though the individual constituent materials of the composite may be strain rate independent. Such a model was discussed earlier by L.M.Barker [51].

Following to Maxwellian model, L.M.Barker has introduced a metastable (instantaneous) and equilibrium stress-strain paths of loading, and stress relaxation from an instant state to the equilibrium one. It is necessary to say that determination of the metastable loading path for composite is a problem. On the other hand, computations and available measurements of shock-wave processes in composite materials do not reveal any signs of the ultimate metastable states.

In this work we tried to describe the process with an empirical constitutive relationship without determination of metastable paths. Instead of metastable states we assume that fast bulk compression produces superfluous pressure in matter which depends on compression rate. Then an establishing the mechanical equilibrium occurs through the superfluous pressure relaxation to zero. Total pressure p is presented as a sum of equilibrium component p_e determined by the equation of state, and nonequilibrium component p_n which depends on the strain rate and load history. Nonequilibrium pressure components at compression were calculated using the empirical kinetic relationship

$$\frac{dP_n}{dt} = K_1 \left(-\frac{t_o}{V_o} \frac{dV}{dt} \right)^n - \frac{P_n}{\tau} \cdot (C/C_o), \qquad (3)$$

where t_o= 1s, K_1, n, and relaxation time τ are the material constants. An acceleration of the reverberation process due to increasing the sound velocity with pressure is taken into account.

The same relationship with a reverse sign at dV is used for rarefaction.

Empirical kinetic relationship (3) contains three parameters: K_1, n, and τ, , which, in principle, can be estimated from series profiles of steady shock waves with different peak pressures. When a steady wave propagates through a material, all parts of the wave propagate with the same constant velocity, and the material, therefore, is loaded along a Rayleigh line to the final state on the equilibrium behavior curve. Intermediate states in the steady compression wave contain some superfluous pressures that equal the difference between stresses at the Rayleigh line and equilibrium pressures corresponding to the material equation of state:

$$p_n = \rho_o U^2 (V_o - V) - p(V); \qquad \dot{p}_n = -\rho_o^2 \dot{V} (U^2 - a^2),$$

where U is the shock front velocity, $a = \left(- V_o^2 \frac{dp}{dV}\right)^{1/2}$ is the Lagrangian sound velocity. In some intermediate point of the shock wave the superfluous stress passes through the maximum. In this point $\dot{p}_n = 0$ and, according to (3),

$$K_1 \tau = P_n^{max} (C/C_o) \left(- \frac{t_o}{V_o} \frac{dV}{dt}\right)^{-n}.$$

Thus the strain rate dependence on the p_n^{max} value give an estimation of the $K_1 \tau$ product and the power index n. A slope of the shock-wave just in the front point, where a superfluous stress is steel zero and sound velocity is C_o, gives us

$$\dot{p}_{no} = -\rho_o^2 \dot{V} (U^2 - C_o^2) = K_1 \left(- \frac{t_o}{V_o} \frac{dV}{dt}\right)^n.$$

Last relationship can be used to find the K_1 value. It shows also the power index n has to exceed unit because in the case of n=1 initial slope of the steady compression wave does not depend on its intensity, and in the case of $n < 1$ the slope decreases with increasing shock intensity.

Results of 1-D simulation with $K_1 = 1.5 \cdot 10^8$ Pa/s, $n = 1.5$, and τ =

$2 \cdot 10^{-8}$ s are compared with 2-D data in Figures 18. Equation of state based on the Hugoniot of mixture was used in 1-D calculation. One can see a sufficient agreement between results of two kinds of calculations.

4.3. CONSTITUTIVE MODEL FOR DYNAMIC RESPONSE OF BRITTLE MATERIALS.

To construct rather simple constitutive model of the brittle material we used as a basis the structural Marzing model [53]. This model reflects a micro-nonuniformity of real materials and is successfully used for the Baushinger effect description at the repeated-alternating loading.

In frame of the Marzing model model each elementary volume of body is represented as consisting from N parallel elastic-viscous-plastic subelements. Subelements have equal elastic modulus, but different yield strengths and viscosities. The stress in each subelement is determined as

$$\sigma = \sum_{1}^{N} \sigma_k \ g_k ,$$

where σ^k are stresses inside the subelements, g_k are weight factors which can be presented as relative areas of subelements cross-sections. Inelastic strain component appears at moment when an yield strength of the weakest subelement is reached. The ultimate stress in this model is

$$\bar{\sigma} = \sum_{1}^{N} Y_k \ g_k .$$

Effective elastic modulus after yield stress reached in n subelements is

$$\bar{E}_{n+1} = E_o \ (1 - \sum_{1}^{n} g_k),$$

where E_o is the elastic modulus of subelements. The model can be generalized on the arbitrary stresses state [53].

For high-strain-rate conditions it is necessary to take into account the viscosity of matter. Measurements of the shock front structure [54] show the shear plastic strain rate in the range of 10^4 to 10^7 s^{-1} is related to shear stress as

$$\dot{\gamma}_p = A' \, (\tau - Y/2)^2,$$

where A' is constant. In frame of the multi-elements model the plastic strain rate of subelements can be calculated as [55]

$$\dot{\gamma}_p^k = A' \, [\frac{\bar{\sigma}}{Y_k} (\tau^k - Y_k /2)]^2,$$

Both strain hardening and softening of subelements describe a complex response of materials to the shock-wave loading.

Most of practical applications of the computer simulations of the brittle materials dynamic response require are associated with three-dimensional analysis. From this point of view it is necessary to avoid superfluous details which can be prohibitively expensive in realization of the computer model. In relation to multi-elements model this means that we have to reduce to minimum the number of elements. In fact, two elements are quite enough to describe with sufficient accuracy the main peculiarities of the material response.

Our model of brittle material includes two parallel elements. One of them works as usual elastic-plastic body, possibly - with strain hardening. Another element describes the resistance to deformation of the comminuted component. For this second element the resistance to shear is a friction. Initially we deal with solid undamaged ceramic, so it is naturally to assume the initial fraction of the comminuted component to be zero. With beginning of an inelastic deforming the brittle material is cracking and the fraction of comminuted component is growing with increasing inelastic strain. After some strain the initial intact material becomes completely failed, that means the fraction of comminuted component reaches 1 and the resistance to shear is determined by friction in a granular material only. Thus in frame of this model the comminuted component fraction is a scalar damage variable which ranges from a value of 0 to 1. In the model the fraction of comminuted components grows with increasing inelastic deformation of intact component:

$$g_2 = \frac{\beta\gamma_p^1}{1 + \beta\gamma_p^1},$$

where γ_p^1 is the inelastic strain of the intact component.

A dilatational effect has been formally incorporated into the model to take into consideration an increase in volumetric strain resulting from cracks growth. In the present model the dilatancy is associated with inelastic deformation of comminuted component and is expressed in terms of increments of relative volume of voids. Obviously shear strains under compression can produce just limited volume of voids. On the other hand, positive pressure above some threshold has to close voids. Basing on these simple ideas we have tried to describe the dilatancy by the following empirical relationship

$$\frac{d\bar{V}_v}{d\gamma_p^2} = \frac{k_1 \, g_2}{1 + k_2 \, V_v} - \left(\frac{p - p^*}{p_o} \right)^2 \bar{V}_v ,$$

where $\bar{V}_v = V_v / V_o$ is the relative volume of voids, γ_p^2 and g_2 are the inelastic deformation and weight factor of the comminuted component, k_1, k_2, p^*, p_o are the material constant parameters. Voids are not closed when pressure does not exceed the threshold value p^*.

The model does not include any degradation of shear module with inelastic compression. The shear module dependence on the pressure is calculated in the approach of constant Poisons ratio which means that ratio of the shear module to the bulk module is not changed with changing pressure and temperature. Yield strength of the intact component is changed proportionally to the shear module. The tensile strength of the matter was supposed to be negligible.

A computer simulation of shock-wave experiments [26,27] with boron carbide ceramic has been performed. The boron carbide ceramic was analyzed because previous calculations [45-49] for this ceramic were lest successful. Results of calculations with our constitutive model are compared with experimental [26,27] velocity profiles in Figure 19. It seems the agreement between results of calculations and experimental data is quite reasonable. Figure 20 shows states of material during shock compression and

unloading. One can see the strong Baushinger effect is described well by the model. The dilatancy effect is most essential at last stages of unloading.

CONCLUSION

Results presented here can be considered as encouraging in sense that way of investigation of the heterogeneous materials response to dynamic loading using the 2-D computer simulation of the phenomena can be really productive. Some important details of the dynamic compression process in composite, porous and brittle materials have been established due to 2-D simulation. Reasonable constitutive relationships were then designed to describe behavior of composites and brittle materials under impact loading. The following work can be directed to more advanced analysis of the deformation process, to development of constitutive models and to finding the models parameters values for some determined materials.

REFERENCES.

1. Composite materials v.2./ Mechanics of Composite Materials. Edited by G.P.Sendeckyj. Academic Press. New York and London, 1974.
2. Achenbach J.D., Herrmann G. Dispersion of Free Harmonic Waves in Fiber-Reinforced Composites. AIAA Journal, v.6, N 10, pp. 1832-1836, 1968
3. Achenbach J.D., Sun C.T. in "Dynamics of composite materials" (Lee E.H. ed.), New York, Amer.Soc.Mech.Eng., 1972, pp.48-69.
4. Hashin Z. Theory of Mechanical Behavior of Heterogeneous Media. Appl.Mech.Rew., N1, 1964
5. O'Donoghue P.E., Friesenhahn G.J., Anderson C.E., Parr C.H. Anisotropic Model Development for Shock Wave Propagation Computer Programs./ Shock Compression of Condensed Matter-1989 / Edit. S.C.Schmidt,J.N.Johnson,L.W.Davison/ Elsevier Science Publishers B.V.,1990, p.181
6. Alekseev Yu. F., Al'tshuler L.V., and Krupnikov V.P.: J.Appl. Mech. and Techn. Phys. (USSR), 1971, No.4, p.152.
7. Duvall G.E. and Taylor S.M. Shock Parameters in a Two Component Mixture: J. Composite Materials, 1971, Vol.5, p.130
8. Bushman A.V., Efremov V.P. et al.: Thermophysics of High Temperatures (USSR), 1990, v.28, No.6, pp1232-1234.
9. Anderson C.E., O'Donoghue P.E., Skerhut D. Anisotropic Model Development for Shock Applications./ Shock Compression of Condensed Matter-1989/Edit. S.C.Schmidt,J.N.Johnson,L.W.Davison/ Elsevier Science Publishers B.V.,1990, p.177.
10. W.Herrrmann. Constitutive Equation for the Dynamic Compaction of Ductile Porous Materials. - J. Appl. Phys., 1969, v. 40, n.6, pp. 2490-2499.
11. R.R.Boade. Experimental Shock-loading Properties of Porous Materials and Analytical Methods to Describe these Properties. - in: "Shock Waves and Mechanical Properties of Solids", ed.: J.J.Burke and V.Weiss, Syracuse University Press, New York, 1971, pp.263-285.
12. M.M.Carroll, A.C.Holt. Suggested Modification of the p-α Model for Porous Materials. - J.Appl. Phys., 1972, v. 43, n.2, p.759 -761.
13. Ki-Hwan Oh and Per-Anders Persson. A Constitutive Model for the Shock Hugoniot of Porous Materials in the Incomplete Compaction

Regime. - J. Appl. Phys., 1989, vol.66, n.10, pp. 4736-4742.

14. M.M.Carroll, A.C.Holt. Static and Dynamic Pore-Collapse Relations for Ductile Porous Materials. - J.Appl. Phys., 1972, v. 43, n.4, p. 1626.
15. B.M. Butcher, M.M.Carroll, and A.C.Holt. Shock-wave Compaction of Porous Aluminum. - J. Appl. Phys., 1974, vol. 45, n.9, pp.3864 - 3874.
16. S.Z. Dunin, V.V. Surkov. The Structure of Shock-Wave Front in the Solid Porous Media. - J. of Appl. Mechanics and Techn. Phys. (USSR), 1979, n.5, pp. 106-114.
17. J.W.Swegle. Constitutive Equation for Porous Materials with Strength. - J. Appl. Phys., 1980, vol. 51, n.5, p. 2574.
18. G.V.Belyakov. Shock Deformation of granular media. - Dokl. Akad. Nauk SSSR, 1974, v. 218, pp. 1280-1282.
19. B.A.Hasainov, A.A.Borisov, B.S.Ermolaev, and A.I.Korotkov. - Seventh Sympos. (Internat.) on Detonation, NSWC MP 82-334, 1981, pp.435-447.
20. B.A.Hasainov, A.A.Borisov, B.S.Ermolaev. - Shock Waves, Explosions and Detonations. Progress in Astronautics and Aeronautics, 1983, vol. 87, pp. 492-504.
21. A.V.Attetkov, L.N.Vlasova, V.V.Selivanov, V.S.Soloiev. - Zh. Prikl. Mekh. Tekh. Fiz., 1984, No 6, p.119.
22. R. Frey. - Eight Sympos. (Internat.) on Detonation, Albuquerque, NM, vol.1, p.385.
23. C.L.Mader. Numerical Modelling of Detonation. University of California Press, Usa, 1979.
24. R.L.Williamson and R.N.Wright. A Particle-Level Numerical Simulationof the Dynamic Consolidation of a Metal Matrix Composite Material.- Shock Compression of Condensed Matter - 1989, Ed.: S.C.Schmidt et al., Els. Sc. Publ. B.V., 1990, pp. 487-490.
25. Brace W.F. Paulding B.W., Sholz C. J.Geophys.Res., 1966, v.71, N16, p.3939.
26. M.E.Kipp and D.E.Grady. Shock Compression and Release in High-Strength Ceramics. Sandia Report SAND89-1461, UC-704, printed July 1989.
27. M.E.Kipp and D.E.Grady. In: Shock Compression of Condensed Matter - 1989. Ed.: S.C.Schmidt, J.N.Johnson, L.W.Davison, Els. Sc. Publ., 1990, p.377.
28. D.Grady. In: Shock Compression of Condensed Matter - 1991. Ed.: S.C.Schmidt, R.D.Dick et al. Els. Sc. Publ., 1992, p.455.

29. Z.Rozenberg. In: Shock Compression of Condensed Matter - 1991. Ed.: S.C. Schmidt, R.D. Dick et al. Els. Sc. Publ., 1992, p.439.
30. Z.Rosenberg, N.S.Brar, and S.J.Bless. In: Shock Compression of Condensed Matter - 1991. Ed.: S.C. Schmidt, R.D. Dick et al. Els. Sc. Publ., 1992, p. 471.
31. D.P.Dandekar. In: High Pressure Science and Technplogy - 1993. Ed.: S.C.Schmidt, J.W.Schaner, et al. American Institute of Physics, AIP Conference Proceedings 309, 1994, p.729.
32. L.Ewart and D.P.Dandekar. In: High Pressure Science and Technplogy - 1993. Ed.: S.C.Schmidt, J.W.Schaner, et al. American Institute of Physics, AIP Conference Proceedings 309, 1994, p.1201.
33. D.P.Dandekar and P.Bartkowski. In: High Pressure Science and Technplogy - 1993. Ed.: S.C.Schmidt, J.W.Schaner, et al. American Institute of Physics, AIP Conference Proceedings 309, 1994, p.733.
34. W.-D. Winkler and A.J.Stilp. In: Shock Compression of Condensed Matter - 1991. Ed.: S.C. Schmidt, R.D. Dick et al. Els. Sc. Publ., 1992, p. 475.
35. L.H.L. Louro and M.A.Meyers. J. Mat. Sci., 1989, vol. 24, p.2516
36. L.H.Leme Louro and M.A.Meyers. In: Shock Compression of Condensed Matter - 1989. Ed.: S.C.Schmidt, J.N.Johnson, L.W.Davison, Els. Sc. Publ., 1990, p.465.
37. Kachanov L.M. Introduction to continuum damage mechanics. Martinus-Nijhof, 1986.
38. DragonA., Mroz Z. Int.J.Engng.Sci., 1979,v.17,p.121
39. Supartono F., Sidoroff F. Arch.Mech., 1985, v.37, N4/5, p.521.
40. Rabotnov U.N. Introduction in fracture mechanics (in Russian), Moscow, Nauka, 1988.
41. Krajcinovic D., Lemaitre J.(ed.) Continuum damage mechanics - Theory and applications, Springer, 1986.
42. Murakami S. Trans.ASME.J.Engng.Mater.Technol., 1983, v.105, N2, p.99.
43. Chaboche J.L. J.Appl.Mech., 1988, v.55, p.59.
44. Huang Z.P.,Yang L.M., Pan K.L. Damage of materials under dynamic loading.-In Recent Progress in Plasticity, 1992, p.139.
45. F.L.Addessio and J.N.Johnson. J. Appl. Phys., 1990, vol. 67 (7), p.3275.
46. D.J.Grove and M.Rajendran. In: High Pressure Science and

Technplogy - 1993. Ed.: S.C.Schmidt, J.W.Schaner, et al. American Institute of Physics, AIP Conference Proceedings 309, 1994, p.749.

47. D.J.Steinberg. In: Shock Compression of Condensed Matter - 1991. Ed.: S.C. Schmidt, R.D. Dick et al. Els. Sc. Publ., 1992, p.447.
48. D.Steinberg, S.Cochran and M.Guinan. J.Appl. Phys., 1980, vol. 51, po. 1498.
49. J.F.Davis, J.R.Furlong and M.Alme. In: Shock Compression of Condensed Matter - 1991. Ed.: S.C. Schmidt, R.D. Dick et al. Els. Sc. Publ., 1992, p.479.
50. Munson D.E. and Schuler K.W. Steady Wave Analysis of Wave Propagation in Laminates and Mechanical Mixtures.: J. Composite Materials, 1971, Vol.5, p. 286
51. Barker L.M.. A Model for Stress Wave Propagation in Composite Materials. : J. Composite Materials, 1971, Vol.5, p.140.
52. Oved Y., Luttwak G.E., and Rosenberg Z. Shock Wave Propagation in Layered Composites. - J. Composite Materials, 1978, Vol.12, p.84.
53. D.A.Gokhfeld and O.S.Sadakov. Plasticity of Structural elements under Repeated Loads. (in Russian). Mashinostroenie, Moscow, 1984.
54. J.W.Swegle, D.E.Grady. - J.Appl. Phys., 1985, vol.58, No.2, p.692.
55. G.I.Kanel. Problems of Strength (USSR), 1988, No 9, p.55.
56. D.J.Steinberg. Equation of State for B_4C and BeO. Lawrence Livermore Laboratory Report LLL-UCID-16946, 1975.

APPENDIX A.

MATHEMATICAL MODEL FOR 2-D COMPUTER SIMULATION

One can hope that computer simulation of the dynamic deformation processes in composite material can make clear details of these processes and find correlation between mechanical properties of material and its components. Some preliminary results were obtained in our previous research.

Calculations are based on fundamental conservation lows [1] and are conducted in Lagrangian material coordinates. Conservation of momentum is described by equations

$$a_x = \frac{\partial U_x}{\partial t} = V\left(\frac{\partial(\Sigma_{xx} - P)}{\partial X} + \frac{\partial \Sigma_{xx}}{\partial X}\right), \qquad (1)$$

$$a_z = \frac{\partial U_z}{\partial t} = V\left(\frac{\partial(\Sigma_{zz} - P)}{\partial X} + \frac{\partial \Sigma_{zz}}{\partial X}\right). \qquad (2)$$

Equation of conservation of energy is

$$\frac{\partial E}{\partial t} = V\left(\frac{\partial I}{\partial X}\right) + V\left(-\frac{P}{V}\frac{\partial V}{\partial t}\right) + V\left(\Sigma_{xx}\dot{e}_{xx} + \Sigma_{zz}\dot{e}_{zz} + \Sigma_{xz}\dot{e}_{xz}\right) + V\left\{\frac{\partial}{\partial X}\left(\lambda\frac{\partial T}{\partial X}\right) + \frac{\partial}{\partial Z}\left(\lambda\frac{\partial T}{\partial Z}\right)\right\}. \qquad (3)$$

The first term in the right part of equation (3) is energy release due to external source; second term is the work of bulk strain; third term is the work of shear strain; fourth term describes the internal energy increment due to thermocondactivity; $\dot{e}_{xx} = \frac{\partial U_x}{\partial X}$, $\dot{e}_{zz} = \frac{\partial U_z}{\partial Z}$, and $\dot{e}_{xz} = \frac{\partial U_x}{\partial Z} + \frac{\partial U_z}{\partial X}$ are strain rates.
The mass conservation is carried out automatically due to Lagrangian variables used.

Elastic-plastic behavior of the material is described by the Hooke's low for strain rates [2]

$$\frac{\partial S_{xx}}{\partial t} = 2G\left(\dot{e}_{xx} - \frac{P}{3V}\frac{\partial V}{\partial t}\right) + \frac{\delta S_{xx}}{\Delta t} \qquad (4)$$

$$\frac{\partial S_{zz}}{\partial t} = 2G\left(\dot{e}_{zz} - \frac{P}{3V}\frac{\partial V}{\partial t} \right) + \frac{\delta S_{zz}}{\Delta t} \qquad (5)$$

$$\frac{\partial S_{xz}}{\partial t} = G\left(\dot{e}_{xz} \right) + \frac{\delta S_{xz}}{\Delta t} \qquad (6)$$

A rotation angle $\Delta\varphi$ of element of media in the x-z plane during small time step Δt is

$$\Delta\varphi = \Delta t \ \mathrm{rot}\ \vec{U} = \frac{\partial U_x}{\partial z} - \frac{\partial U_z}{\partial x}.$$

Corresponding corrections in equations (4)-(6) are calculated as [3]

$$\delta S_{xx} = (S_{zz} - S_{xx})\sin^2\Delta\varphi + 2S_{xx}\sin\Delta\varphi\ \cos\Delta\varphi$$

$$\delta S_{zz} = - \delta S_{xx}$$

$$\delta S_{xz} = (S_{zz} - S_{xx})\sin\Delta\varphi\ \cos\Delta\varphi + 2S_{xx}\sin^2\Delta\varphi$$

Yielding is tested using Mises criterion. According to this criterion, when

$$f = 2\ (S_{xx}^2 + S_{xz}^2 + S_{zz}^2 + S_{xx}S_{zz}) > \frac{2}{3}\ Y_o^2, \qquad (7)$$

where Y is yield strength, yielding has occurred and the deviator stresses are reduced in the usual way [8]:

$$S_{xx} := S_{xx}\left(\frac{2}{3I} \right)^{1/2} Y_o\ , \qquad (8)$$

$$S_{xz} := S_{xz}\left(\frac{2}{3I} \right)^{1/2} Y_o\ , \qquad (9)$$

$$S_{zz} := S_{zz}\left(\frac{2}{3I} \right)^{1/2} Y_o\ . \qquad (10)$$

A scalar artificial viscosity is used to damp nonphysical oscillations. Combination of the linear q_1 and square q_2 viscosities is used in our code:

$$q_1 = q_1 + q_2\ , \qquad (11)$$

where

$$q_1 = - C_1 A \bullet \Delta l\ \dot{V}/V\ , \qquad (12)$$

$$q_2 = C_2 \Delta l^2 \dot{V}^2 / V \ , \qquad (13)$$

$\Delta l = \sqrt{4 A^2 / b}$ is a characteristic size of the Lagrangian mesh [1], A is the mesh area, b is the sum of the squares of the mesh sides, $\dot{V} = \left(\frac{1}{V} \frac{\partial V}{\partial t} \right)$ is the dilatation rate, $C_1 \approx 0{,}5$ and $C_2 \approx 2{,}0$ are constant coefficients. Artificial viscosity is set equal to zero when dilatation rate is positive.

Natural viscosity has been included into the model in form [4]. The bulk viscosity is described as

$$q_e = -\left(\xi + \frac{2}{3} \eta \right) \dot{V}. \qquad (14)$$

q_1 and q_e values are added to pressure in eqs. (1)-(3). Deviator components of viscous stress are [4]

$$q_{xx} = 2\eta \left(\dot{e}_{xx} - \frac{1}{3} \dot{V} \right) \ , \qquad (15)$$

$$q_{zz} = 2\eta \left(\dot{e}_{zz} - \frac{1}{3} \dot{V} \right) \ , \qquad (16)$$

$$q_{xz} = 2\eta \, \dot{e}_{xz} \ . \qquad (17)$$

In order to damp oscillations of stress components, deviator pseudoviscosities have been introduced into the code also as a combination of the linear [3] and square [1] regarding strain rates terms.

Components of the deviator of the linear pseudoviscosity tensor are

$$q'_{xx} = C_3 \, a \, \Delta l \, \dot{e}_{xx} / V, \quad q'_{zz} = C_3 \, a \, \Delta l \, \dot{e}_{zz} / V,$$

$$q'_{xz} = C_3 \, a \, \Delta l \, \dot{e}_{xz} / V \ ,$$

and components of the deviator of square pseudoviscosity are

$$q''_{xx} = C_4 \, \Delta l^2 \, \dot{e}_{xx} H / V \ ,$$

$$q''_{zz} = C_4 \, \Delta l^2 \, \dot{e}_{zz} H / V \ ,$$

$$q''_{xz} = C_4 \, \Delta l^2 \, \dot{e}_{xz} H / V \ ,$$

where $H = 2\sqrt{J_2}$ is the shear strain rate intensity, $J_2 = (\dot{e}_{xx} - \dot{e}_{zz})^2/6 + 3/2\ \dot{e}_{xz}^2$ is the second invariant of the strain rates deviator, $C_1 \simeq 0{,}5$, and $C_2 \simeq 2{,}0$ are constants. A total pseudoviscosity is sum of linear and square components:

$$\tilde{q}_{xx} = q'_{xx} + q''_{xx} ,$$

$$\tilde{q}_{zz} = q'_{zz} + q''_{zz} ,$$

$$\tilde{q}_{xz} = q'_{xz} + q''_{xz} ,$$

Components of deviator of visco-elastic stresses in eqs. (1)-(3) are determined as

$$\Sigma_{xx} = S_{xx} + q_{xx} + \tilde{q}_{xx} ,$$

$$\Sigma_{zz} = S_{zz} + q_{zz} + \tilde{q}_{zz} ,$$

$$\Sigma_{xz} = S_{xz} + q_{xz} + \tilde{q}_{xz} .$$

An equation of state of the matter was used in form of ref. [4] with correction in field of small densities. The pressure at specific volume $V < V_o$ is calculated using Hugoniot of matter:

$$P = P_H + \frac{\gamma}{V}(E - E_H) , \qquad (18)$$

where $P_H = C_\alpha^2(V_0 - V)/[V_0 - S_\alpha(V_0 - V)]^2$ and $E_H = P_H(V_0 - V)/2$ are pressure and energy on the Hugoniot.

For moderate pressures in a range of approximately 0.5 to 50 GPa, a difference between the Hugoniot and isentrope of the matter is not significant [5]. A temperature in this region $V < V_0$ is

$$T = T_H + (E - E_H)/C_v ,$$

where the temperature on the Hugoniot T_H is calculated as [8]

$$T_H = T_o e^{\gamma(V_o - V)} + \frac{(V_o - V)P_H}{2C_v} -$$

$$- \left[\frac{e^{-\gamma V/V_o}}{2C_v} \right] \int_{V_o}^{V} P\, e^{-\gamma V/V_o} \left[2 - \frac{\gamma}{V} (V_o - V) \right] dV$$

A pressure in field of specific volumes more than initial one ($V > V_0$) is calculated using the Gruineisen equation of state

$$P = \frac{\gamma}{V} (E - E_s) , \qquad (19)$$

where

$$E_s = (B K_{corr})/\gamma (V_o - V)$$

$$K_{corr} = e^{-((V/V_o)^2 - 1)} , \qquad (20)$$

$$\gamma = 2/3 + (\gamma_o - 2/3) K_{corr} .$$

The correcting factor K_{corr} decreases the bulk modulus value B from B_o at $V = V_o$ (what corresponds to usual initial conditions) to zero. By this way the energy of tension of the condensed matter E_s is reduced to zero at $V \to \infty$ affording a smooth transfer to the gas state region. The relationship (20) for K_{corr} is constructed by such a way that E_s value becomes negligible at $V = (3 \div 5) V_o$ [6].

The temperatures in region of $V > V_0$ is

$$T = T_o + E/C_v .$$

Calculation of the heat capacity as a function of temperatures $C_v = f(T)$ is done in the Debye's approach [7]:

$$C_v = 3\, nk\, [4\, D(x) - 3\, x/(e^X - 1)] ,$$

where $D(X) = \frac{3}{x^3} \int_0^x \frac{x^3 dx}{(e^X - 1)}$ is Debye's integral, $X = \theta/T$, θ is the Debye's temperature. The Debye's integral is calculated using standard tables with linear interpolations. The Debye's temperature θ is assumed to be function of the volume only and is calculated as [8]:

$$k\theta = [1,68/(Z + 22)]\ [\rho^{\phi+2}/(1+\rho)^{z}] \qquad [eV],$$

where $\rho = V_{ref}/V$, $\phi = 0,6Z^{1/9}$, $V_{ref} = 0,009\ Z^{0,3}/W$,
Z is the atom number, W is the atom weight.

The set of equations (1) - (3) is solved by the finite differences method on the Lagrangian triangular greed.

REFERENCES

1. Theoretical bases and construction of numerical algorithms for problems of mathematical physics./Edited by K.I.Babenko. Moscow, Nauka, 1979 (in Russian).
2. Wilkins M.L. Cflculation of elsto-plastic flows./Methods in computational physics. Advances in research and applications. Vol.3. Fundamental methods in hydrodynamics./Edited by B.Alder, S.Fernbach, M.Rotenberg. Academic Press. New York and London.
3. Maenchen G., Sack S. Vtthod of calculation "Tensor"./Methods in computational physics. Advances in research and applications. Vol.3. Fundamental methods in hydrodynamics./Edited by B.Alder, S.Fernbach, M.Rotenberg. Academic Press. New York and London.
4. C.L.Mader. Numerical modeling of detonations. University of California Press. Berkeley-Los Angeles-London,1979.
5. Emplosion physics./Edited by K.P.Stanjukovich. Moscow, Nauka, 1975 (in Russian).
6. Zel'dovich Ya.B.,Raizer Yu.P. Physics of Shock Waves and High-Temperature Hydrodynamic Phenomena, Academic Press, New York and London, 1966.
7. McQueen R.G., Marsh S.P., Taylor J.W., Fritz J.N., Carter W.J. State equation of solid by results of shock-wave investigation. /High-Velocity Impact Phenomena./ Edited by R.Kinslow. Academic Press New York and London, 1970.
8. More R.M., Warren K.H., Young D.A., Zimmerman G.B. A new quotidian equation of state (QEOS) for hot dense matter. // Phys.Fluids, 1988, v.31, N10, pp.3059-3078.

APPENDIX B. SIMPLE CODES.

A series of simple codes for personal IBM-compatible computers has been created to estimate an equation of state of composites and to test constitutive relations. All codes have been written in FORTRAN and presented in diskette.

B.1. MIXTURE is a code to calculate Hugoniots of mechanical mixtures through known Hugoniots of components. It works together with the file "HUGS.DAT" which contains Hugoniots of series of materials. You can include any additional Hugoniots into HUGS.DAT file using the same format. In this case you have also to change the number in first position of the "hugs.dat" file (amount of Hugoniots in the list). To use this code just do run it and follow to questions. The system of units is SI.

B.2. MIXSOUND is a code to calculate the sound velocity as a function of the content of components in a mixture. It works with the "HUGS.DAT" file too.

B.3. EOS is a code to check an equation of state which was used in 1-D calculations. It is the equation of state of the Mie-Gruneisen type. The cold compression isentrope is calculated through the Hugoniot of matter basing on coinciding of the Hugoniots and isentrope in the pressure - particle velocity coordinates:

$$p_c = \frac{\rho_o C_o^2}{4S} \left[exp\left(4S \frac{V_o - V}{V_o}\right) - 1 \right],$$

where C_o, S are coefficients of the linear relationship between shock velocity and particle velocity. The Gruneisen parameter is assumed to be constant. This simple equation of state gives enough good description of compressibility of solids and sound velocity near the Hugoniot. Results of calculations with EOS show variations of the Gruneisen parameter along Hugoniot when this equation of state is used.

B.4. COMPOS is 1-D Lagrangian code used to check constitutive relation which describes a wave dispersion in composites. It works

together with COMPINST file where all parameters of calculations are established. COMPINST contains commentaries to all parameters.

B.5. DUBRI is 1-D Lagrangian code to calculate shock-wave processes in the system impactor-target-window. Three different materials can be included in calculations and each of them can be ductile or brittle. This code works together with the file "PARAMS" where all necessary parameters are installed. The system of units is SI. Commentaries to parameters are given in the PARAMS file. The elastic-plastic properties of materials are described by the structural Marzing model which has been presented in part 4.3 of this report. Two parallel elastic-plastic elements have been incorporated into the code.

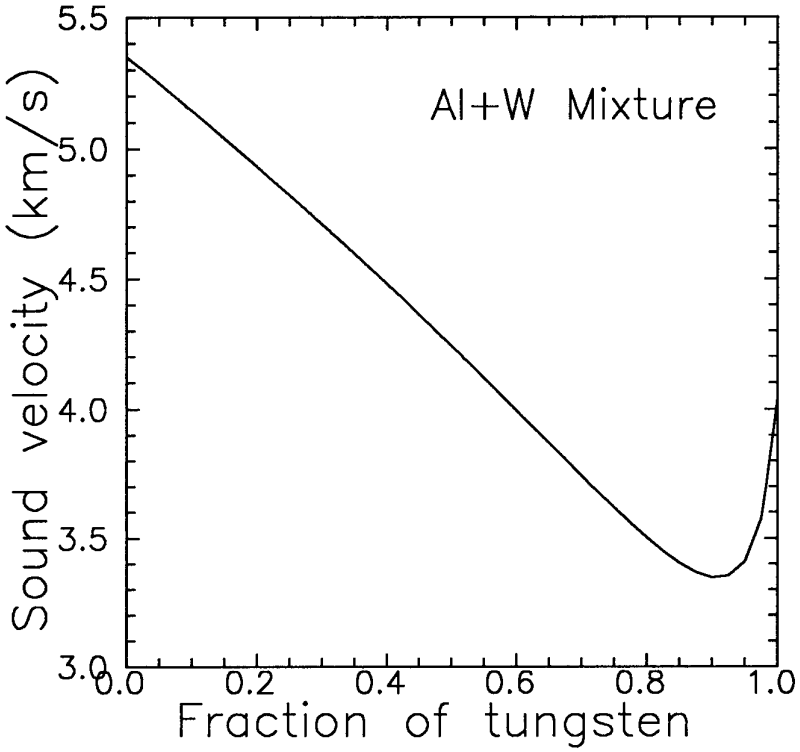

Figure 1. Sound velocity in the aluminum and tungsten mixture calculated in additive approach.

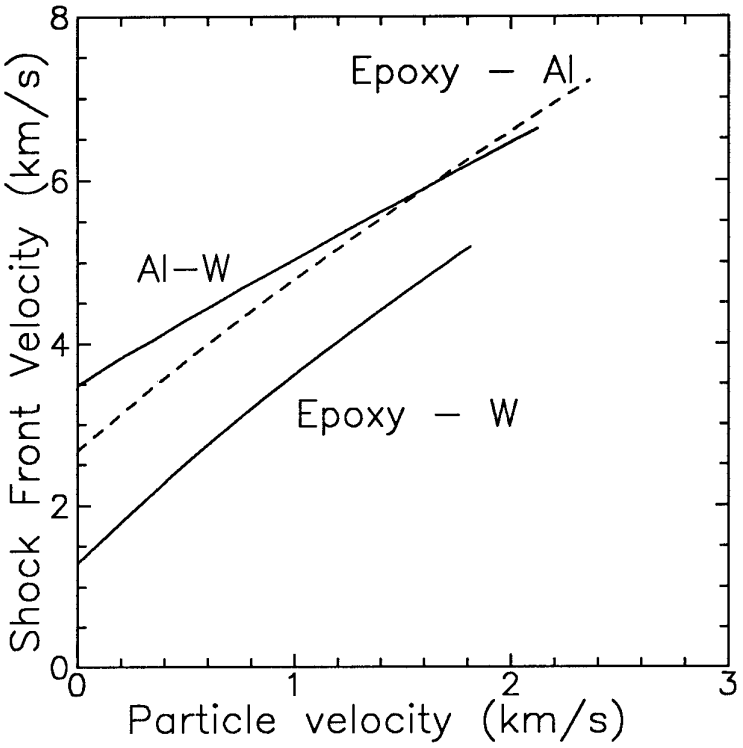

Figure 2. Hugoniots of mechanical mixtures of tungsten with aluminum, tungsten with epoxy, and aluminum with epoxy. Volume fraction of heavy component is 0.375.

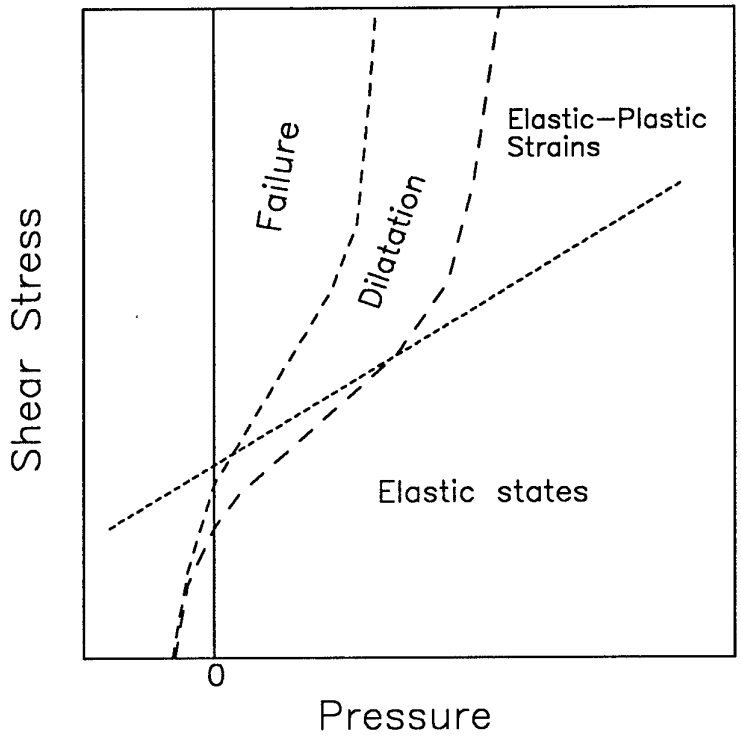

Figure 3. Modes of deformation of a brittle material.

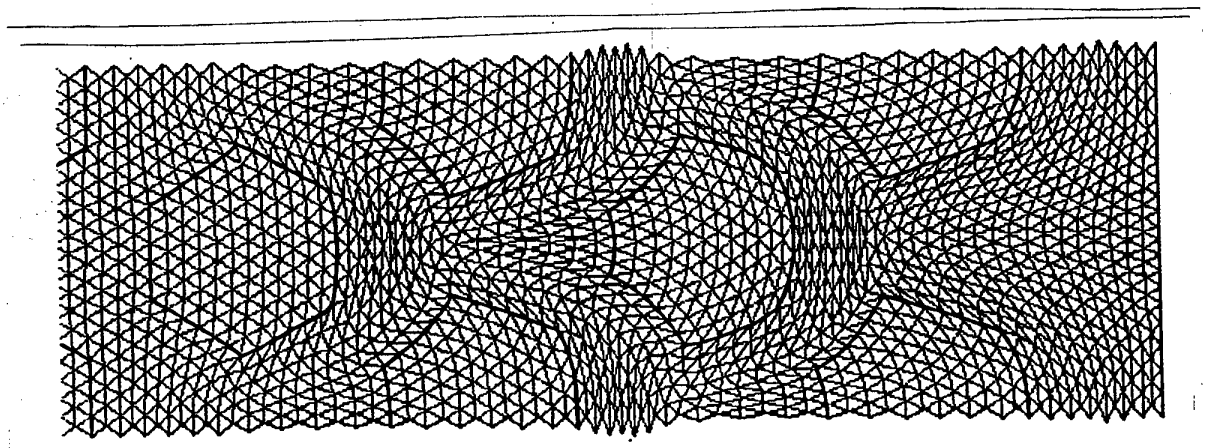

Figure 4. Deformation of the composite material in shock wave. Boundary velocity is 1 km/s.

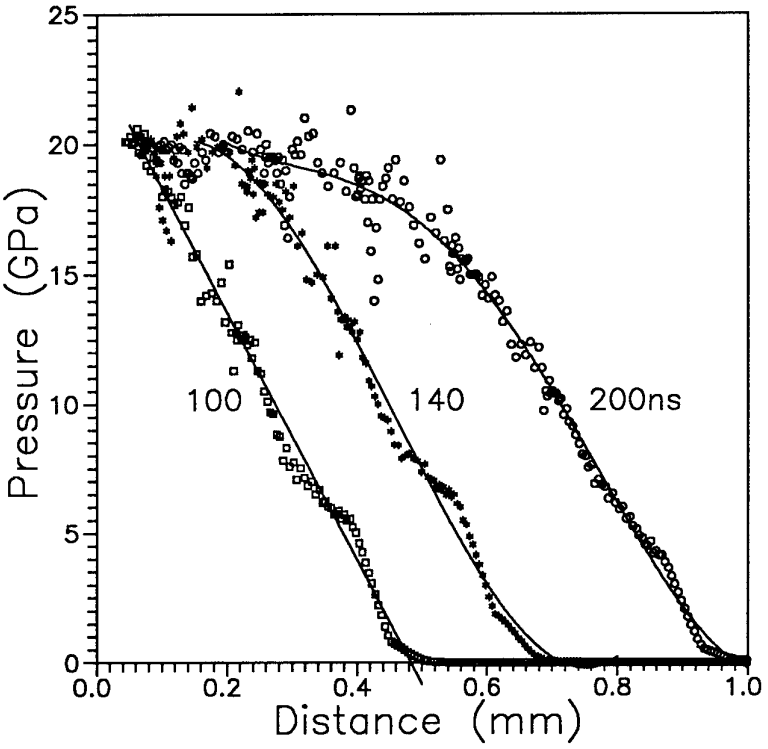

Figure 5. A stress wave evolution in composite at 100 ns of the initial rise time. Hydrodynamic approach.

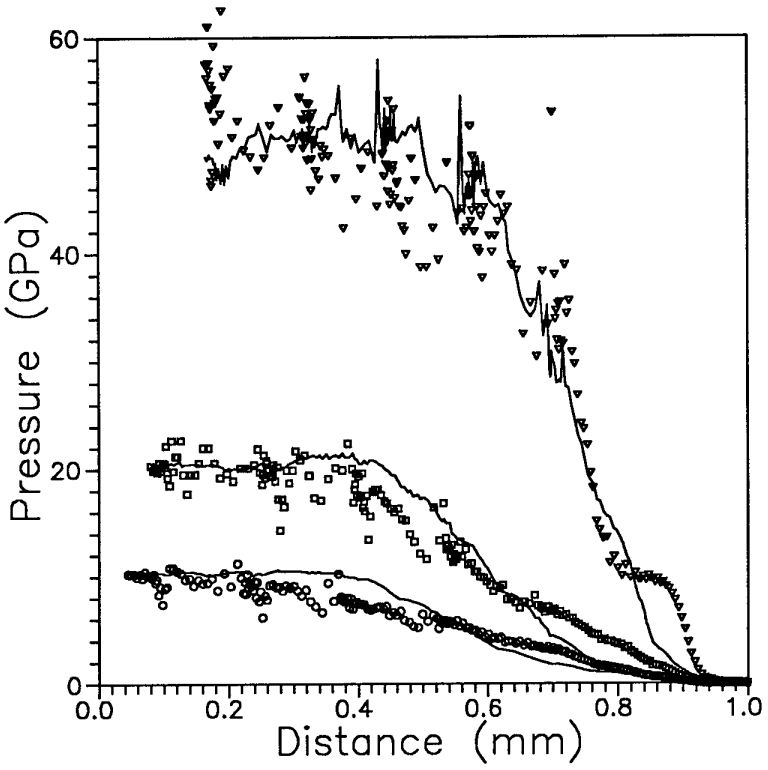

Figure 6. Comparison of the shock-wave stress profiles in the composite calculated in hydrodynamic (points) and elastic-plastic (lines) approaches.

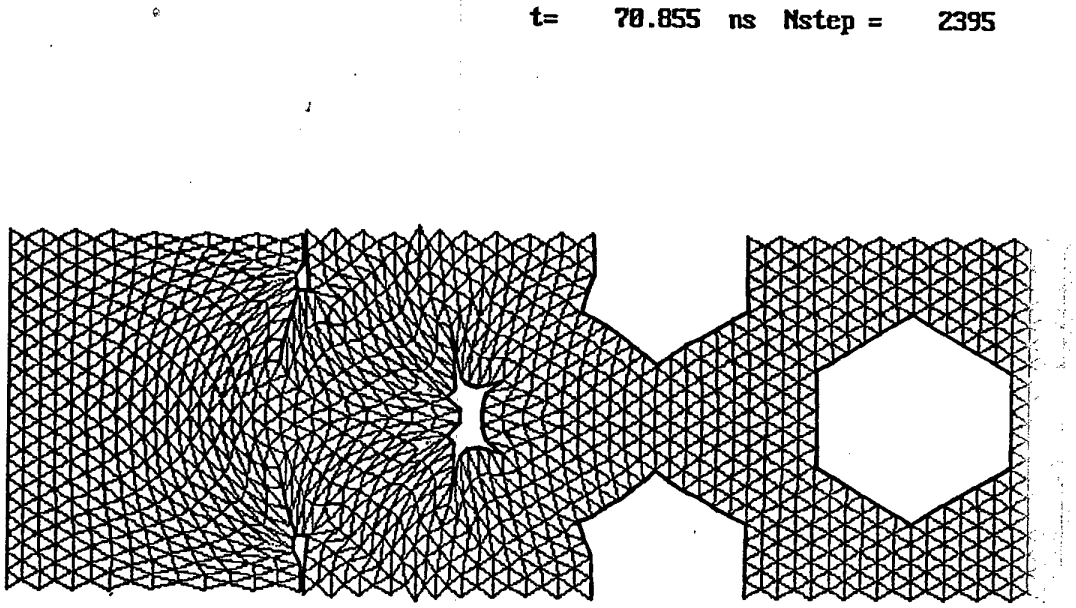

Figure 7. Shock compression of porous aluminum.

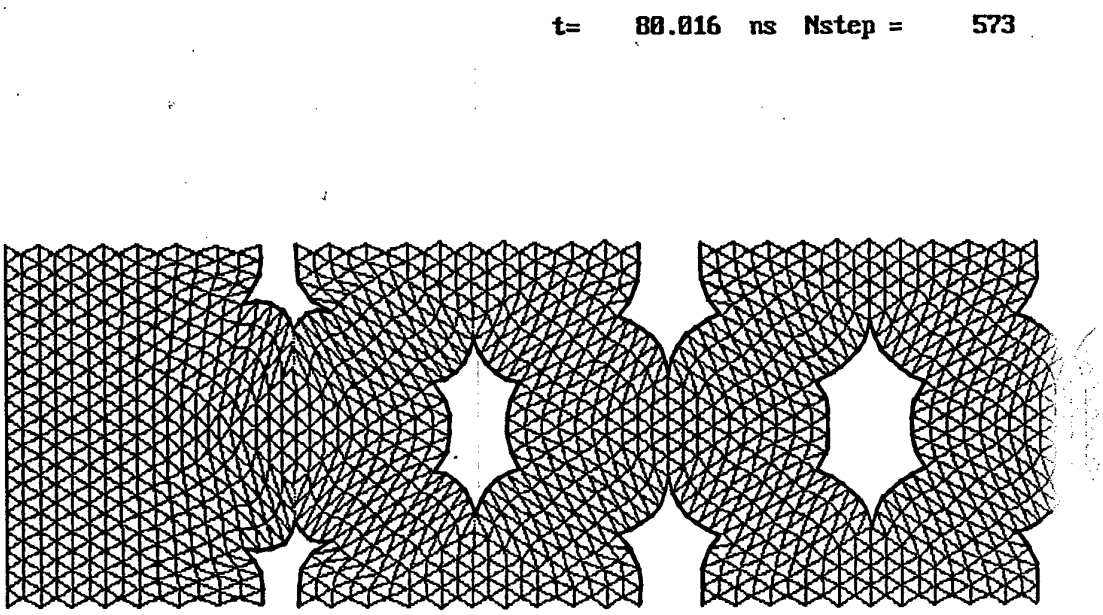

Figure 8. Uniform dynamic compression of porous tungsten at 1 km/s of boundary velocity.

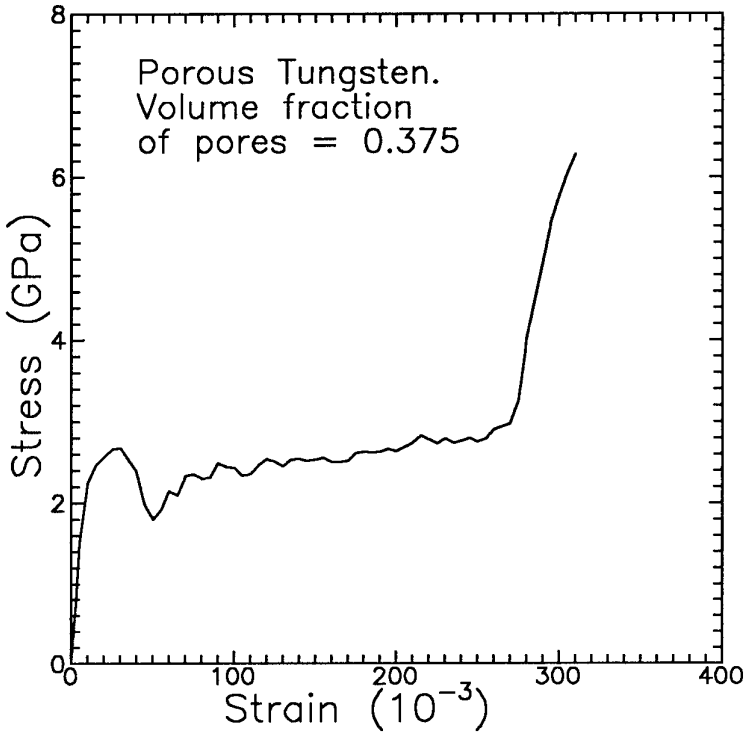

Figure 9. Average stresses in porous tungsten as a function of the strain at uniform dynamic compaction.

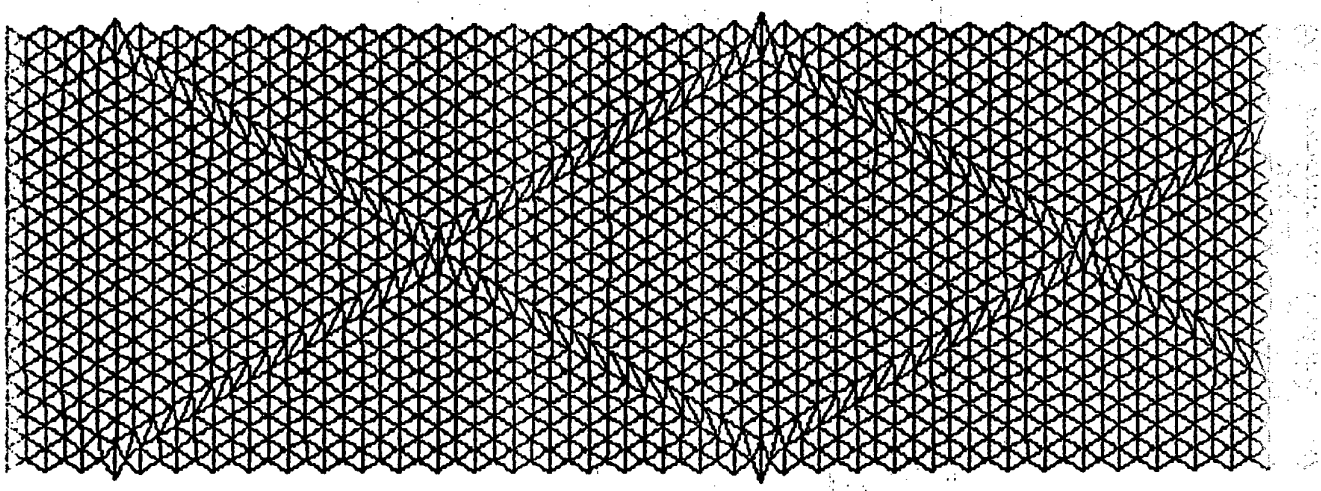

Figure 10. Shock compression of hard ceramic with shear bands.

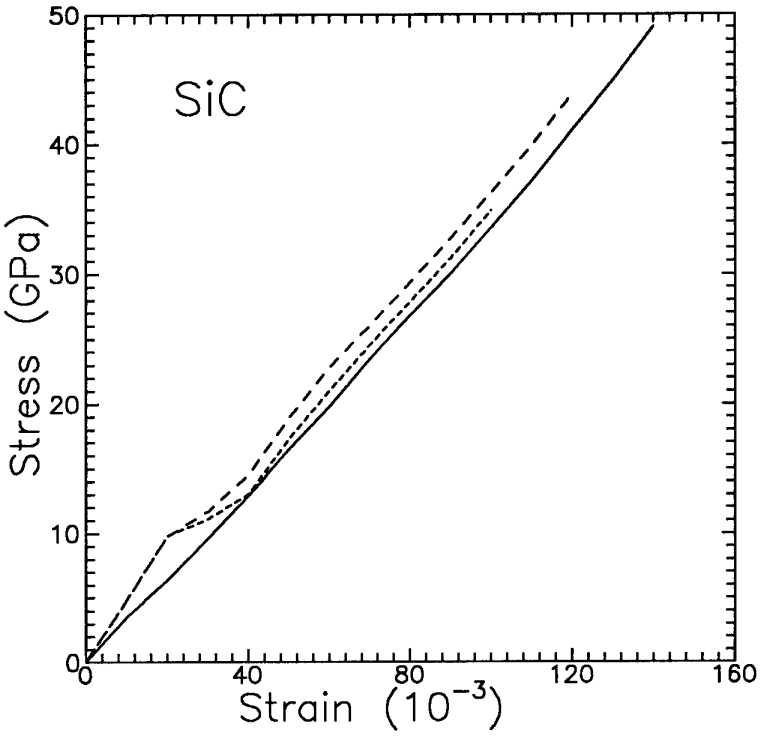

Figure 11. Average stresses in the hard ceramic as a function of strain at the uniform dynamic compression. Friction coefficient was varied from 0 to 0.33.

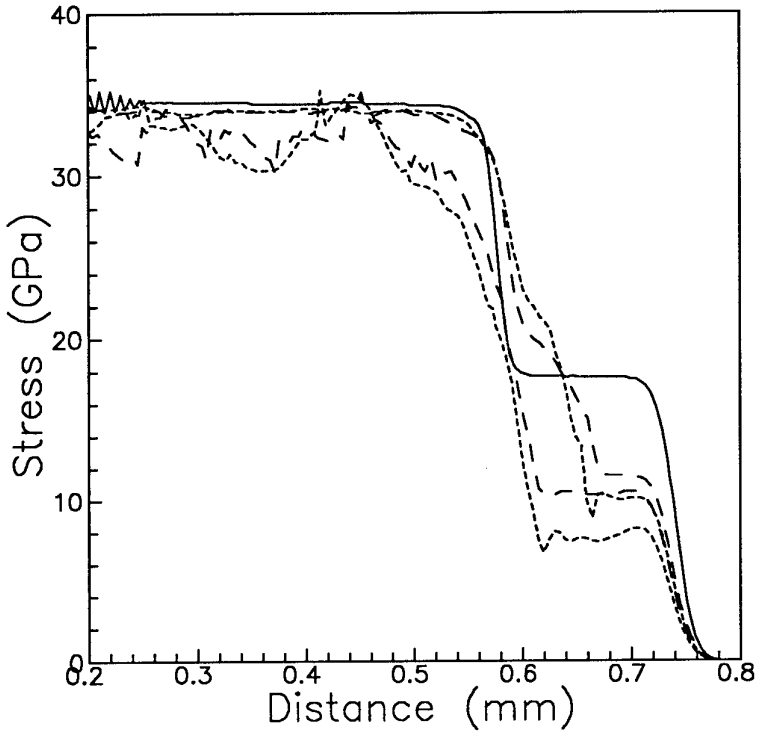

Figure 12. Compression wave profiles in hard ceramic as a result of 2-D simulation. Solid line shows the elastic-plastic approach. Dotted lines show results of calculations with intersecting shear bands. In case of the dashed lines the shear bands were not intersected.

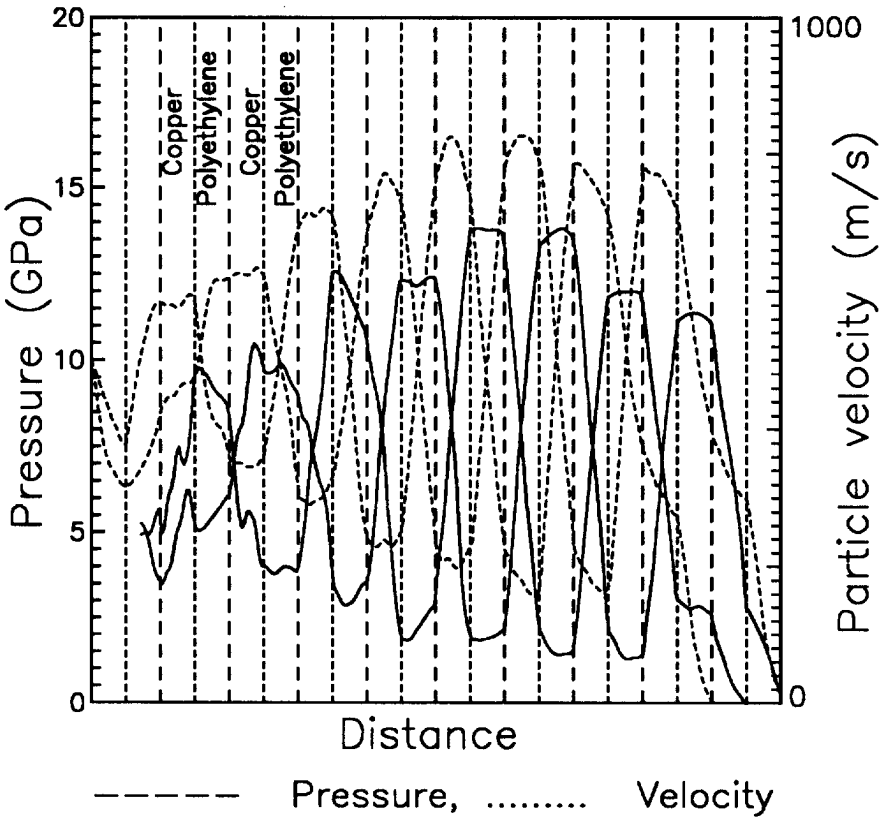

Figure 13. Pressure and particle-velocity oscillations in one-dimensional model of the composite material.

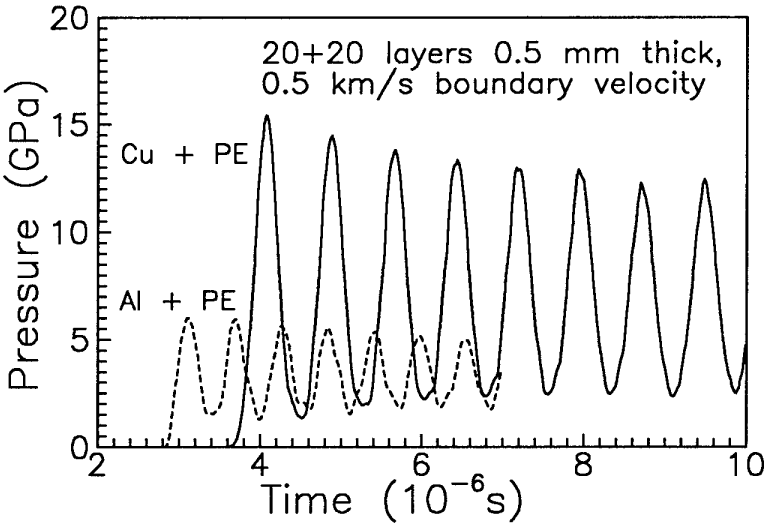

Figure 14. Pressure histories in the middle sections of two layered composites.

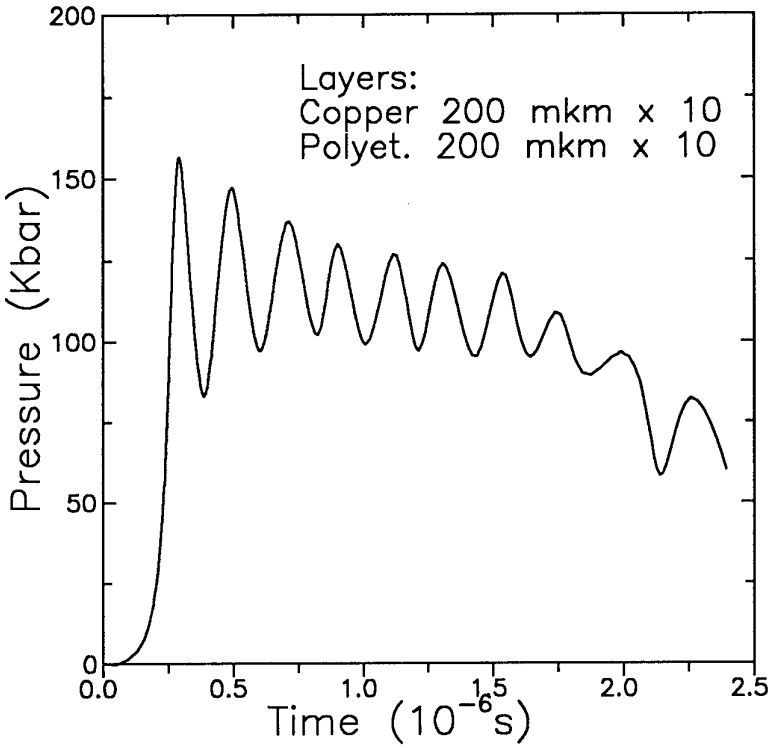

Figure 15. Results of the pressure profile measurement with manganin gauge at the interface between the layered copper-polyethylene composite and a copper plate.

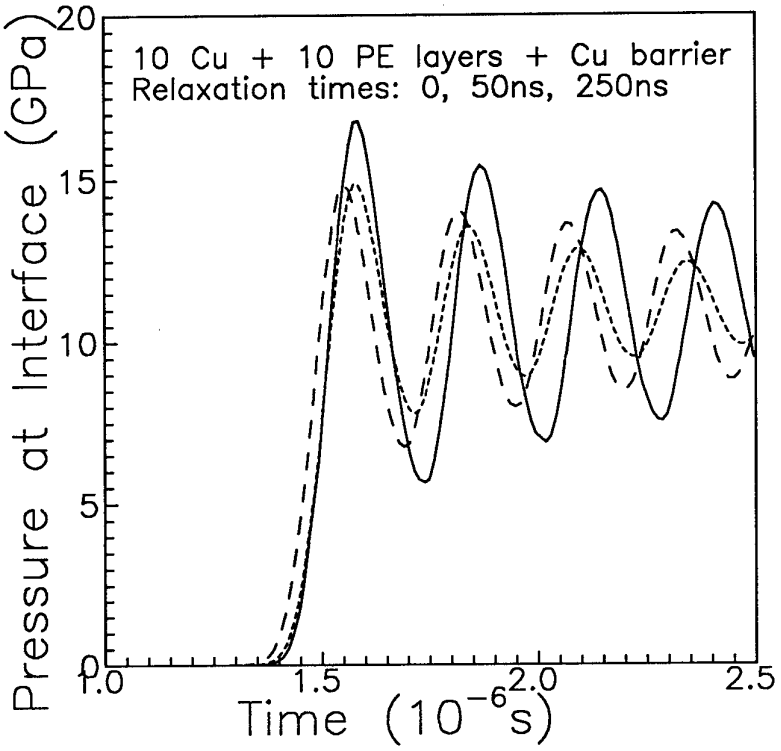

Figure 16. An influence of stress relaxation in polyethylene of the layered copper-polyethylene composite on the pressure profile at the interface with a copper barrier.

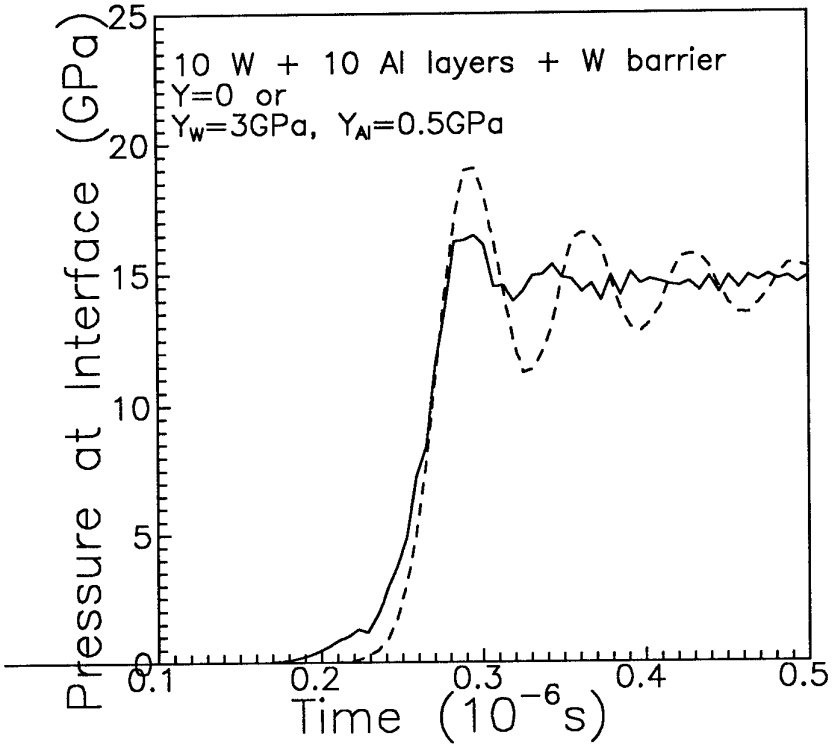

Figure 17. An influence of elastic-plastic properties of the layered aluminum-tungsten composite on the pressure profile at interface with a tungsten barrier.

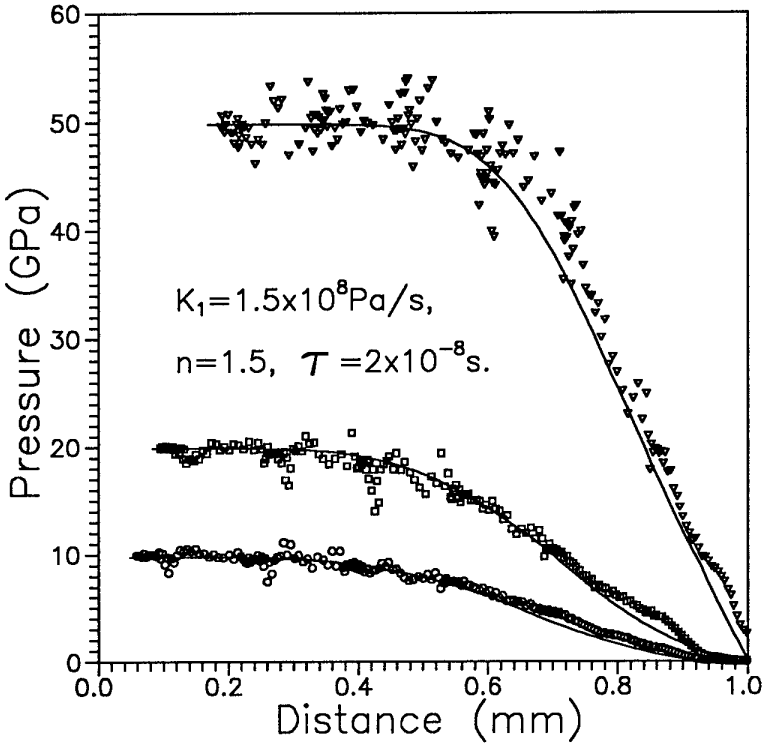

Figure 18. Comparison of 2-D (points) and 1-D (lines) simulations of shock waves in the composite.

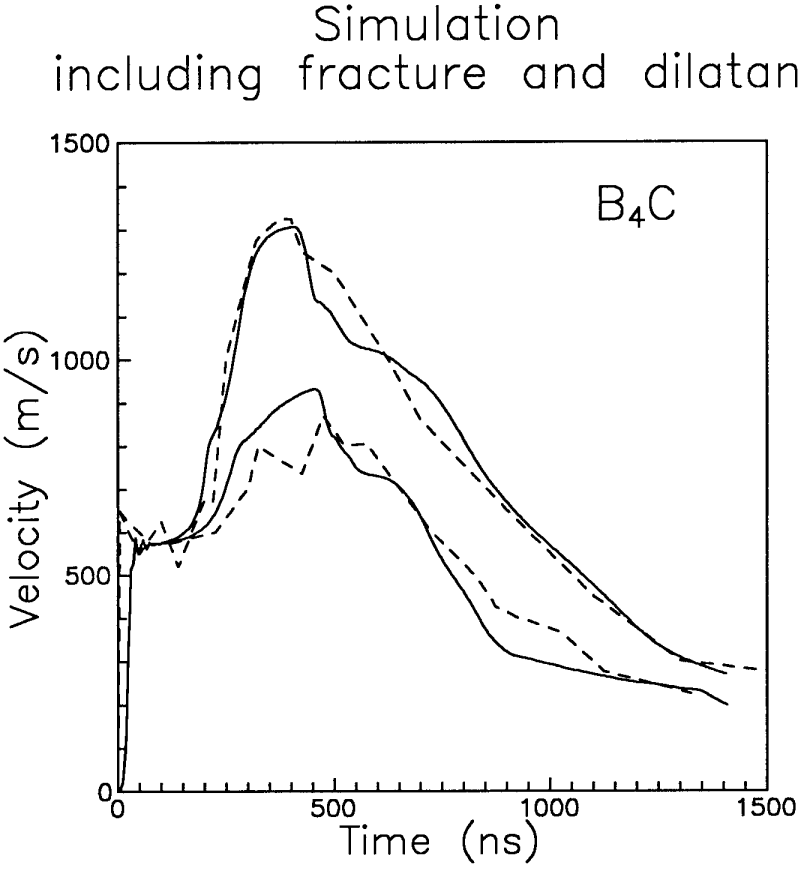

Figure 19. Simulated (solid lines) and measured (dashed lines) particle velocity profiles at shock compression of the boron carbide ceramic.